Cell Stem Cell
Article

The Emergence of Hematopoietic Stem Cells Is Initiated in the Placental Vasculature in the Absence of Circulation

Katrin E. Rhodes,[1] Christos Gekas,[1] Yanling Wang,[1] Christopher T. Lux,[5] Cameron S. Francis,[1] David N. Chan,[1] Simon Conway,[5] Stuart H. Orkin,[6,7,8] Mervin C. Yoder,[5] and Hanna K.A. Mikkola[1,2,3,4,*]
[1]Department of Molecular, Cell and Developmental Biology
[2]Eli and Edythe Broad Center for Regenerative Medicine and Stem Cell Research
[3]Jonsson Comprehensive Cancer Center
[4]Molecular Biology Institute
University of California, Los Angeles, Los Angeles, CA 90095, USA
[5]Herman B. Wells Center for Pediatric Research, Indiana University School of Medicine, Indianapolis, IN 46202, USA
[6]Department of Pediatric Oncology, Dana-Farber Cancer Institute
[7]Howard Hughes Medical Institute
[8]Harvard Stem Cell Institute
Boston, MA 02115, USA
*Correspondence: hmikkola@mcdb.ucla.edu
DOI 10.1016/j.stem.2008.01.001

SUMMARY

The mouse placenta was unveiled as an important reservoir for hematopoietic stem cells (HSCs), yet the origin of placental HSCs was unknown. By tracking developing HSCs by expression of Runx1-lacZ and CD41, we have found that HSCs emerge in large vessels in the placenta. Analysis of *Ncx1*$^{-/-}$ embryos, which lack a heartbeat, verified that HSC development is initiated in the placental vasculature independent of blood flow. However, fewer CD41+ hematopoietic cells were found in *Ncx1*$^{-/-}$ placentas than in controls, implying that some HSCs/progenitors colonize the placenta via circulation and/or HSC emergence is compromised without blood flow. Importantly, placentas from *Ncx1*$^{-/-}$ embryos possessed equal potential to generate myeloerythroid and B and T lymphoid cells upon explant culture, verifying intact multilineage hematopoietic potential, characteristic of developing HSCs. These data suggest that, in addition to providing a niche for a large pool of HSCs prior to liver colonization, the placenta is a true site of HSC generation.

INTRODUCTION

Regeneration of blood cells throughout the lifetime of an individual is dependent upon HSCs and their ability to self-renew and differentiate into all blood lineages (Weissman, 2000). Of all stem cells, HSCs have had the greatest therapeutic impact on human disease, specifically in leukemia and aplastic anemia (Bordignon, 2006). However, due to the shortage of matching donors for transplantation and the low yield of HSCs in more accessible sources such as cord blood, many patients are unable to benefit from this therapy (Cairo and Wagner, 1997). Attempts to expand HSCs in vitro have failed due to loss of self-renewal ability and a propensity to differentiate in culture, highlighting the importance of the microenvironment in the maintenance of stem cell properties. Likewise, derivation of functional HSCs from human embryonic stem cells has not yet been achieved, as the in vitro-derived hematopoietic progenitors poorly self-renew in vivo (McKinney-Freeman and Daley, 2007). To succeed in these endeavors, basic research on how fetal microenvironments support the development of self-renewing HSCs is essential.

Although defining the stem cell niche for adult HSCs has become an extensive area of research and both the cellular and molecular components of the niche are being unraveled, fetal HSC niches have proven highly complex and their unique molecular features remain relatively undefined (Martinez-Agosto et al., 2007). HSCs in adult mice reside in the bone marrow, in the endosteal surface of trabecular bone, and in the vascular sinusoids (Adams and Scadden, 2006; Kiel and Morrison, 2006; Suda et al., 2005; Wilson and Trumpp, 2006; Zhang et al., 2003). During embryogenesis, HSCs migrate through a number of anatomical sites that likely impart unique cues to the cells as they transition through different developmental stages (Mikkola and Orkin, 2006). The development of HSCs begins when mesodermal precursors become specified to the hematopoietic fate in a process that is dependent on the bHLH transcription factor SCL/Tal-1, whereas subsequent establishment of the definitive hematopoietic program and emergence of HSCs requires the core binding factor *Runx1/AML* (reviewed in Teitell and Mikkola, 2006). Of note, newly formed HSCs are not equivalent to adult HSCs, as they require a maturation process before they can engraft into adult bone marrow and self-renew (Mikkola and Orkin, 2006; Yoder et al., 1997a, 1997b). Furthermore, in contrast to relatively quiescent adult HSCs, fetal HSCs are highly proliferative as they expand to establish a supply of HSCs for adult life (Bowie et al., 2006; Kim et al., 2007; Lessard et al., 2004). Thus, both the cell-intrinsic regulatory mechanisms that

govern developing HSCs and the microenvironmental niches where HSCs reside evolve during embryogenesis. To understand the impact of the microenvironment in establishing HSC properties, it is critical to define the cellular niches that support the emergence, maturation and expansion of HSCs.

The first embryonic hematopoietic cells, the primitive erythroblasts, are generated after gastrulation in the yolk sac, as is a second wave of myelo-erythroid progenitors (Lux et al., 2007; Palis et al., 1999). HSCs capable of engrafting newborn mice are found in the yolk sac and para-aortic splanchnopleure (P-Sp) within the embryo proper as early as E9.0 (Yoder et al., 1997a), whereas the first HSCs that possess adult repopulating capability are found in the aorta-gonad-mesonephros (AGM) region of the embryo proper slightly later, after E10.5 (Cumano et al., 1996; Jaffredo et al., 2005; Medvinsky and Dzierzak, 1996). During subsequent days, definitive hematopoietic progenitors and HSCs colonize the fetal liver. However, the low number of HSCs found in the AGM and the extended developmental time that elapses before a substantial number of HSCs have colonized the liver raised the question of whether HSCs may also be generated in the yolk sac and/or in other yet unidentified sites (Kumaravelu et al., 2002). Work by us and others subsequently showed that the mouse placenta harbors a large population of HSCs during midgestation (Alvarez-Silva et al., 2003; Gekas et al., 2005; Ottersbach and Dzierzak, 2005). The placental HSCs appear as early as in the AGM region and before any HSCs had colonized the liver or were circulating in the blood. The placental HSC pool continues to grow, ultimately harboring 15-fold more HSCs as compared to the AGM. As the placental HSC population declines, the liver HSC pool expands, suggesting that the placenta may be a major source of the HSCs that seed the liver (Gekas et al., 2005). These findings nominated the placenta as an important hematopoietic organ, unique in its capacity to sustain a large pool of HSCs while segregating them from signals that promote differentiation. However, these studies did not determine whether the placenta is capable of producing HSCs de novo or whether it functions solely as a niche for the maturation and expansion of HSCs originating from other sites.

Defining the origin of HSCs in vivo has been complicated by circulation and the limitations of functional assays for developing HSCs. Once a heartbeat is initiated at E8.5, any cell within the vasculature may be released into circulation. Although free distribution of progenitors is delayed until E10.5 (McGrath et al., 2003), adult repopulating HSCs are found only after this time and may therefore have circulated from other sites. Because developing HSCs are unable to engraft in lethally irradiated adult bone marrow before day E10.5, one cannot directly assay HSC potential in the earlier tissues with the standard in vivo assays. As transient embryonic progenitors with restricted myelo-erythroid potential develop prior to the emergence of HSCs, documentation of multilineage differentiation ability, including lymphoid potential, is essential to distinguish developing HSCs from transient embryonic hematopoietic progenitors.

As all hematopoietic cells are derived from mesoderm, tracking the fate of the mesodermal tissues is critical when origin of hematopoietic cells is being explored. The placenta is comprised of trophectoderm and two mesodermal components: the chorionic mesoderm, which forms a continuum with the yolk sac, and the allantoic mesoderm, an appendage arising from the posterior primitive streak. The allantoic mesoderm migrates toward the ectoplacental cone, fuses with the chorion, and intertwines with the trophoblast to form the placental vascular labyrinth, which facilitates the exchange of nutrients, gas, and minerals between mother and fetus (Cross, 2005; Inman and Downs, 2007). Interestingly, earlier studies on quail-chick chimeras showed that the avian allantois is a source of definitive hematopoietic cells (Caprioli et al., 1998, 2001). Recently, the hematopoietic potential of the mouse chorionic and allantoic mesoderm was assessed (Corbel et al., 2007; Zeigler et al., 2006) by in vitro culture of the tissue explants that were harvested prior to chorio-allantoic fusion and circulation. Strikingly, these studies documented myelo-erythroid hematopoietic potential in both the allantoic and chorionic mesoderm, supporting the hypothesis that HSCs may be generated in the placenta. Yet, these studies did not assess lymphoid potential of the rudiments. Of note, one study in 1979 described B lymphoid potential in the midgestation placenta; however, the origin of these cells was not defined (Melchers, 1979).

Our goal was to determine whether the mouse placenta is a true site of HSC generation and identify the cellular niches in which placental HSCs reside. By using the *Runx1*-lacZ and *Ncx1* knockout mouse models, we demonstrate that definitive hematopoiesis is autonomously initiated in the placenta. As the $Ncx1^{-/-}$ embryos lack a heartbeat due to a defect in the sodium calcium exchanger 1 (Koushik et al., 2001), our data verify without input from circulating cells that HSC potential is present in the placenta. The placental-derived hematopoietic cells were capable of producing both myelo-erythroid and B- and T lymphoid progeny, fulfilling the criterion of multipotentiality that is the defining feature of developing HSCs. The process of HSC emergence is always intimately associated with the large vessels in the placenta. Furthermore, the small vessels in the placental labyrinth may serve as a niche where HSCs convene for maturation and expansion prior to seeding the fetal liver.

RESULTS

Runx1 Transcription Factor Marks the Onset of Definitive Hematopoiesis

To identify developing HSCs and define the cellular niches that support HSCs in the placenta, we used the *Runx1*-lacZ knockin mouse model. *Runx1* is essential for the emergence of definitive HSCs and remains expressed in HSCs throughout fetal development and adult life (North et al., 2002). As in other hematopoietic tissues, Runx1 expressing cells in the placenta coexpressed markers of developing HSCs. (Figure S1 available online). In $Runx1^{lacZ/+}$ embryos, which have only one targeted allele, HSCs develop in all hematopoietic organs. Although the kinetics of HSC development has been reported to be slightly altered due to *Runx1* haploinsufficiency (Cai et al., 2000), localization of Runx1-lacZ+ cells has been used to identify developing HSCs and their niches. In contrast, HSC generation is abolished in $Runx1^{lacZ/lacZ}$ and $Runx1^{lacZ/-}$ embryos, which have both *Runx1* alleles targeted. However, the activity of the *Runx1* locus persists in the null embryos and drives the expression of the lacZ reporter, marking the sites where *Runx1* dependent definitive hematopoiesis is initiated (North et al., 2002).

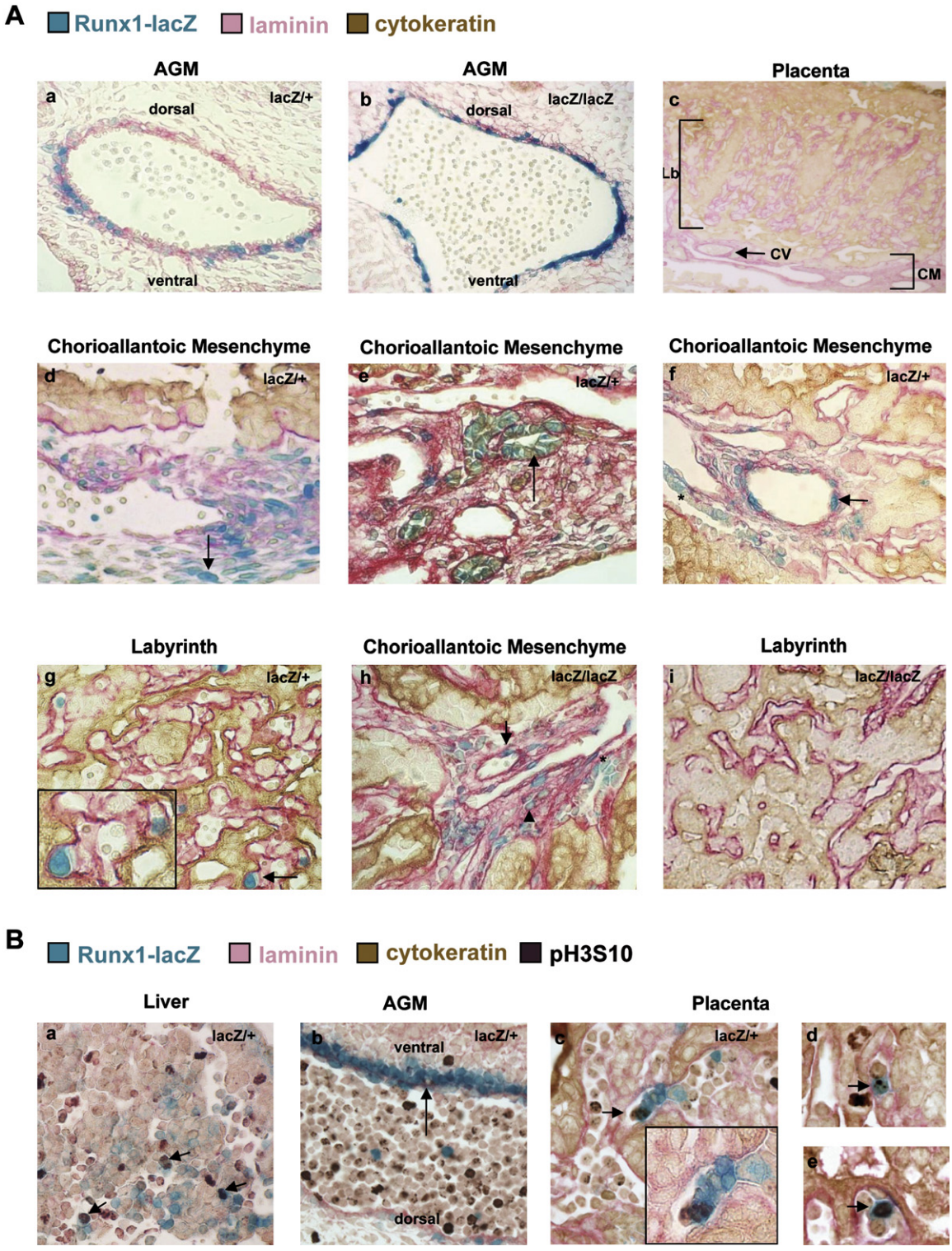

Figure 1. Runx1 Expression Marks the Sites of Definitive Hematopoiesis in the Placenta

Paraffin sections stained with β-galactosidase (lacZ, blue), laminin (mesodermal derivatives, red), and cytokeratin (trophoblast and epithelial cells, brown). (A) Runx1-lacZ+ cells in the dorsal aorta in the (a) *Runx1*$^{lacZ/+}$ and (b) *Runx1*$^{lacZ/lacZ}$ embryos mark a known site of HSC emergence (E11.5, 40X). (c) Section from E11.5 placenta illustrates the specific regions in the placenta: chorioallantoic vessels (CV) in the chorioallantoic mesenchyme (CM) connect to the umbilical cord (data not shown), whereas the labyrinth (Lb) consists of fetal vessels, trophoblasts, and maternal blood spaces, providing the site for fetal-maternal exchange (5×). (d) In *Runx1*$^{lacZ/+}$ placentas, oblong lacZ+ cells (arrow) were resident in the chorioallantoic mesenchyme (40X). (e) At E11.5, lacZ+ cuboidal cells (arrow), which ultimately form the Crypt of Duval, present as tubular structures in the chorioallantoic mesenchyme. (f) Chorioallantoic vessels of *Runx1*$^{lacZ/+}$ placentas

In the AGM, an established site of HSC emergence, lacZ+ cells were localized to the dorsal aorta in both the heterozygous (*Runx1*$^{lacZ/+}$) and null (*Runx1*$^{lacZ/lacZ}$ and *Runx1*$^{lacZ/-}$) embryos (Figures 1Aa and 1Ab). Although Runx1-lacZ+ cells were more prominent in the ventral side of the aorta, in some sections lacZ+ cells circumscribed the entire aorta. In contrast to the AGM, the liver does not generate HSCs de novo but functions as a site of expansion and differentiation for definitive hematopoietic cells seeded from other sources. Accordingly, lacZ+ hematopoietic cells had colonized the liver in *Runx1*$^{lacZ/+}$ embryos, but not in the *Runx1*$^{lacZ/lacZ}$ embryos (data not shown).

In *Runx1*$^{lacZ/+}$ placentas, multiple lacZ+ cell types were found. Oblong-shaped lacZ+ cells were scattered in the chorioallantoic mesenchyme that surrounds the large placental vessels (Figure 1Ad). The chorioallantoic mesenchyme also harbored cuboidal cells that stained for lacZ and cytokeratin (Figure 1Ae). These cells are derived from ectoplacental endoderm and form structures called Crypts of Duval (Duval, 1891; Ogura et al., 1998). At E10.5–11.5, lacZ+ cells were also found integrated in the wall of the chorioallantoic vessels, reminiscent of lacZ+ cells in the AGM (Figure 1Af). Finally, round lacZ+ cells, which sometimes were arranged in small clusters, were found within the lumen of the labyrinth vessels between E10.5 and E12.5 (Figure 1Ag).

Interestingly, *Runx1*$^{lacZ/lacZ}$ placentas revealed similar populations of oblong lacZ+ cells in the mesenchyme and endothelial-like lacZ+ cells integral to the wall of the large chorioallantoic vessels (Figure 1Ah), suggesting that these lacZ+ cells may be the precursors that would give rise to HSCs if Runx1 were present. In contrast, in the null, lacZ+ cells were never found in the lumen of the labyrinth vasculature (Figure 1Ai), implying that the labyrinth lacZ+ cells in the *Runx1*$^{lacZ/+}$ placentas are fully emerged definitive hematopoietic cells. Cytokeratin+lacZ+ Crypts of Duval were also prevalent in the *Runx1*$^{lacZ/lacZ}$ placentas (Figure 1Ah).

To investigate whether placental microenvironment stimulates proliferation of HSCs, cells undergoing mitosis were identified with an antibody specific to phosphorylated serine 10 at histone 3 (pH3S10). As expected, pH3S10 colocalized with lacZ+ hematopoietic cells in the *Runx1*$^{lacZ/+}$ liver (Figure 1Ba). In contrast, in the AGM, PH3S10 rarely colocalized with the abundant lacZ+ cells attached to the ventral wall of the dorsal aorta (Figure 1Bb). Interestingly, in *Runx1*$^{lacZ/+}$ placentas, mitotically active lacZ+ cells were found in the labyrinth vessels, occasionally forming clusters with other lacZ+ cells (Figures 1Bc–1Be). In contrast, the lacZ+ cells in the chorioallantoic mesenchyme were rarely dividing (data not shown). These findings point to the placental labyrinth vessels as a microenvironment that supports expansion of definitive hematopoietic cells.

CD41 Expression Defines Localization of Candidate HSCs in Placental Vasculature

As Runx1 expression is not restricted to HSCs, known markers for nascent HSCs and differentiated blood cells were utilized to verify hematopoietic identity. Previously, we and others have described CD41 (integrin alpha2b, GpIB) as a marker for nascent HSCs and progenitors (Corbel and Salaun, 2002; Ferkowicz et al., 2003; Matsubara et al., 2005; Mikkola et al., 2003; Mitjavila-Garcia et al., 2002). After E11.5, CD41 expression declines in HSCs and is restricted to megakaryocytes/platelets and some progenitors. Although CD41 expression in the placenta has not yet been studied as extensively as in other hematopoietic sites, our data show that all myelo-erythroid clonogenic progenitors and most robust B lymphoid potential of E10.5–11.0 placentas reside in the CD41+ fraction (Figure S2). As expected, a high degree of colocalization of Runx1 and CD41 expression was shown by FACS analysis of hematopoietic tissues of *Runx1*-GFP embryos and IHC analysis of *Runx1*-lacZ embryos (Figure S1). Interestingly, CD41+ hematopoietic cells were confined to the vasculature and were never found in the chorioallantoic mesenchyme underneath the vessels. As early as E9.5–10.5, placental CD41+ cells were found within the wall of the chorioallantoic vessels protruding into the vessel lumen (Figures 2Aa and 2Ab) and then became prominent in the lumen of the vessels in the mesenchyme and the developing labyrinth (Figures 2Ab and 2Ac). Of note, CD41+ maternal platelets were found in the trophoblast-lined maternal spaces, whereas fetal platelets appeared after E10.5 in placental and embryonic vasculature. In the AGM, CD41+ cells were also associated with the dorsal aorta or other vessels in the trunk (Figure 2Ca), and we have previously reported CD41+ hematopoietic clusters in the yolk sac vasculature (Ferkowicz et al., 2003; Mikkola et al., 2003). Although these results do not reveal the origin of the precursor of the CD41+ hematopoietic cells, these studies do highlight the vasculature in the placenta, the embryo proper, and the yolk sac as the sites in which definitive hematopoietic cells may first appear.

To define whether the chorioallantoic mesenchyme stroma harbors other hematopoietic cells, placentas were screened for a panel of hematopoietic markers. Ter119+ red blood cells were found solely in the fetal and maternal blood spaces (data not shown). In contrast, many cells in the chorioallantoic mesenchyme expressed F4/80, a macrophage marker (Figure 2Ba). Serial sections and costainings showed that some F4/80+ cells coexpressed the pan-hematopoietic marker CD45 and monocyte-macrophage marker Mac1 (Figure 2Bb and data not shown). These results suggest that a primitive macrophage population, distinct from CD41+ nascent definitive HSCs and adult macrophages that always express CD45, develops in placental mesenchyme. Absence of F4/80+ macrophages in the chorioallantoic mesenchyme of the *Runx1*$^{lacZ/lacZ}$ and *Runx1*$^{lacZ/-}$ placentas verified that the macrophages are of fetal, not maternal, origin (data not shown). F4/80 macrophages were also found in the yolk sac, at the junction where the yolk sac connects with the placenta, and the mesenchyme surrounding the umbilical cord and the dorsal aorta (data not shown and Figure 2Cb).

harbor lacZ+ candidate HSCs (arrow) within the vessel wall. Asterisk (*), Crypt of Duval. (g) Labyrinth vessels of the *Runx1*$^{lacZ/+}$ placenta harbored a number of lacZ+ cells (E11.5, 40×, 100×). (h) *Runx1*$^{lacZ/lacZ}$ placentas had lacZ+ cells incorporated into the wall of chorioallantoic vessels (arrow) and in the surrounding mesenchyme (arrowhead). Asterisk (*), Crypt of Duval (E11.5, 40×). (i) However, *Runx1*$^{lacZ/lacZ}$ labyrinth vessels never contained lacZ+ cells (E11.5 40X).
(B) Colocalization of Runx1-lacZ expression and pH3S10 (dark purple/brown), a marker of mitosis, in (a) *Runx1*$^{lacZ/+}$ fetal liver documents expected proliferation of definitive hematopoietic cells (E11.5, 40X). (b) In the AGM, lacZ+ cells rarely colocalized with pH3S10 (E10.5, 20×). (c–e) The placental labyrinth vessels harbored lacZ+ cells (arrow) that costained with pH3S10 (E10.5, 40×, 100×).

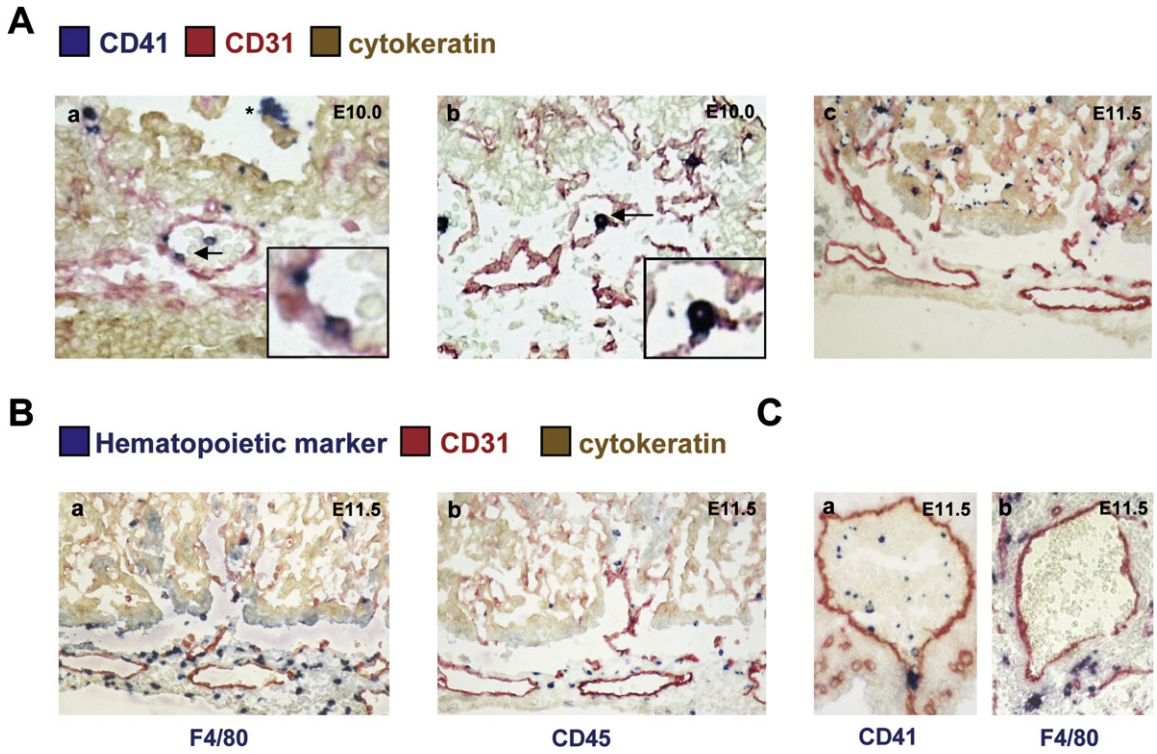

Figure 2. Definitive Hematopoietic Cells and Macrophages Segregate into the Vascular and Stromal Compartments of the Placenta

Fixed frozen sections stained with hematopoietic markers (blue), CD31 (endothelium, red), and cytokeratin (trophoblasts, brown).

(A) (a and b) In wild-type placentas, CD41+ nascent definitive hematopoietic cells (arrows) were integrated into the chorioallantoic vessels (E10.0, 20×, 100×). Asterisk (*), maternal platelets. (c) At E11.5, CD41+ cells populated the labyrinth (E11.5, 10×).

(B) (a) F4/80+ macrophages populate the placental mesenchyme (E11.5, 10×). (b) Some cells in the mesenchyme expressed the pan-hematopoietic marker CD45 (E11.5, 10×).

(C) (a) Rare CD41+ cells (arrow) emerge from the ventral wall of the dorsal aorta (E11.5, 10×). (b) F4/80+ macrophages localize to the mesenchyme surrounding the dorsal aorta (E11.5, 10×).

Ncx1$^{-/-}$ Embryos Document the Emergence of Definitive Hematopoietic Cells in the Placental Vasculature in the Absence of Circulation

To verify whether the HSCs found in the placenta are generated in situ or are merely imported via circulation, we utilized the *Ncx1* knockout mouse model. *Ncx1*$^{-/-}$ embryos have no heartbeat due to a defect in the sodium-calcium exchange pump 1 and do not survive beyond E10.5 (Koushik et al., 2001). As trafficking of hematopoietic cells between tissues via the bloodstream is abolished in the absence of a heartbeat, *Ncx1*$^{-/-}$ embryos provide a unique model in which to assess de novo hematopoietic potential in individual sites. Importantly, Ncx1 is not expressed in hematopoietic cells, eliminating the possibility of cell-autonomous defects (Lux et al., 2007).

At E8.5, *Ncx1*$^{-/-}$ embryos were indistinguishable from control littermates (*Ncx1*$^{+/+}$ and *Ncx1*$^{+/-}$), whereas from E9.5 onward, mutant embryos were pale due to lack of circulating blood cells (Figure 3A). Ter119+ primitive erythroblasts were observed in the yolk sac, where they are generated, in both control and *Ncx1*$^{-/-}$ embryos (Figure 3B). Although placental vasculature had started to develop in the *Ncx1*$^{-/-}$ embryos independent of the physical forces associated with blood flow, the endothelial-lined fetal blood spaces were devoid of circulating erythroblasts, whereas the trophoblast-lined spaces were filled with smaller maternal red blood cells (Figure 3Cb). Strikingly, immunohistochemical analysis showed emergence of CD41+ nascent hematopoietic cells in *Ncx1*$^{-/-}$ placentas in the same locations as in the wild-type placentas, coupled with the vessels of the chorioallantoic mesenchyme and developing labyrinth. Occasionally, CD41+ cells formed clusters that were connected to the vessels (Figures 3Ea–3Ed). Although CD41+ cells were less frequent in *Ncx1*$^{-/-}$ placentas than in wild-type controls (on average 2.2 CD41+ cells in *Ncx1*$^{-/-}$ placental section versus 13.6 CD41+ cells in control section), the mutants frequently displayed prominent CD31+ cell aggregates consisting of round cells that were found protruding into the lumen of the vessels (Figures 3Cb and 3Ed). In umbilical cord, a proposed site of HSC emergence (de Bruijn et al., 2000), a similar aggregate of CD31+ cells contained CD41+ hematopoietic cells (Figure 3Ed). It is possible that these aggregates represent hemogenic intermediates that accumulate in the mutant in the absence of blood flow.

Placenta-Derived Hematopoietic Cells Exhibit Myelo-Erythroid and Lymphoid Differentiation Potential

As the *Ncx1*$^{-/-}$ embryos become developmentally retarded and die by E10.5, further assessment of HSC development in vivo

was not possible. In order to verify that hematopoietic cells in the *Ncx1*$^{-/-}$ placentas are capable of multilineage differentiation, we assessed their potential in vitro. Hematopoietic tissues were harvested between E8.5 and E9.5 to assay their developmental potential without possible acquisition of secondary defects due to the lack of circulation. Hematopoietic potential was assayed on OP9 and OP9-DL1 stroma that support myelo-erythroid, B-, and T lymphoid differentiation (Figure 4A) (Schmitt and Zuniga-Pflucker, 2002). The placentas in control and *Ncx1*$^{-/-}$ embryos generated mixed hematopoietic outgrowth in culture, including definitive progenitors that expressed c-Kit and CD41 (Figure 4B). Similar populations developed also from dissociated yolk sac and caudal half explants (data not shown). When the myelo-erythroid differentiation potential of the progenitors obtained by the explant culture was assayed on methylcellulose, *Ncx1*$^{-/-}$ tissues generated erythroid, myeloid, and mixed colonies, similar to controls (Figure 4C and Figure S3B). PCR genotyping revealed that these colonies are of fetal, not maternal, origin (Figure 4D). Culture of *Ncx1*$^{-/-}$ tissues on growth conditions that promote B lymphoid development generated an abundant B220+ population from all three hematopoietic organs (Figure 4E). As CD19 expression in B cells derived from the tissue explants in these culture conditions was low, genomic PCR of B cell-specific IgH locus rearrangements was performed and confirmed by sequencing (data not shown). Furthermore, when cultured on OP9-DL1 stroma that supports T lymphoid differentiation, all three hematopoietic tissues generated T lymphoid cells that ranged from immature T cell (CD44+/−CD25+/−) precursors to more mature T cells (CD4+/−CD8+/−) (Figure 4F). Although E9.0–9.5 embryos were used in most studies, comparable results were obtained from the analysis of tissues from E8.5–8.75 embryos, isolated right after chorioallantoic fusion when circulation is first initiated. Of note, at this stage, the allantois/developing umbilical cord and the placenta were analyzed as one unit, whereas at E9.5, the umbilical cord was dissected out to verify that the hematopoietic potential was in the placenta proper. When the yolk sac was analyzed, the vitelline vessels were not separated, and therefore we cannot discern where in the yolk sac/vitelline vasculature HSCs arise. Taken together, these data show that, in addition to the AGM and the yolk sac, the placenta is capable of de novo generation of multipotential definitive hematopoietic cells that can differentiate into myeloid, erythroid, and lymphoid lineages, indicative of developing HSCs.

DISCUSSION

The origin of hematopoietic stem cells has remained a focus of intense research, and the model of fetal hematopoiesis continues to evolve as new hematopoietic sites are discovered. Our goal was to assess whether the placenta, a recently discovered fetal hematopoietic organ, generates definitive HSCs de novo. Using the *Runx1*-lacZ and *Ncx1* knockout mouse models, we found that definitive hematopoietic cells encompassing both myelo-erythroid and lymphoid potential are generated in the placenta. Emergence of HSCs is closely associated with the large vessels of the placenta, reminiscent of the process that occurs in the dorsal aorta and the vitelline and umbilical arteries. These studies imply that the conception of HSCs extends to a much larger anatomical area than was previously thought. Furthermore, our data suggest that the vascular network in the placental labyrinth may provide a unique hematopoietic niche that is conducive to the proliferation of hematopoietic cells and serves as a supportive niche for a large pool of HSCs prior to liver colonization.

The cellular origin of the HSC has been debated for decades (reviewed in Jaffredo et al., 2005). One theory posits that HSCs arise from hemogenic endothelium, where specialized endothelial cells generate clusters of hematopoietic cells that bud into the vascular lumen. An alternative theory proposes that a mesodermal precursor, peripheral to the vasculature, is specified for hematopoietic lineage before crossing the endothelial wall to the vascular lumen (Bertrand et al., 2005). Localization of Runx1 expression in the placenta did not define whether the precursor to the HSC resides within the endothelial wall or subvascular mesenchyme, as lacZ expression was found in both sites in the *Runx1*$^{lacZ/+}$ and *Runx1*$^{lacZ/lacZ}$ embryos (Figure 1), and other cells in addition to HSCs express Runx1. Interestingly, we found that the subvascular mesenchyme was populated by macrophages, whereas CD41+ nascent definitive hematopoietic cells always appeared within the vessels. Further studies will be required to define where the precursors for definitive hematopoietic cells and macrophages arise. Expression of endothelial markers CD31, VE-Cadherin, and CD34 in HSCs has been implicated as evidence of a close developmental ancestry between HSCs and endothelial cells (Fraser et al., 2002; Taoudi et al., 2005; Yoder et al., 1997a). Interestingly, the *Ncx1*$^{-/-}$ placentas frequently displayed large aggregates of CD31+ cells that were protruding into the lumen. As these aggregates were not found in the controls, it is likely that they form due to lack of developmental signals normally conveyed by blood flow. It is possible that they are comprised of precursors to definitive hematopoietic cells that are stalled during their emergence into the vascular lumen. Indeed, the CD31+ aggregates consist of round cells that are morphologically similar to hematopoietic cells, and cells in one of the clusters in the umbilical cord also expressed CD41. Alternatively, they may represent endothelial cells that are unable to organize properly in the absence of blood flow. Mechanical forces created by circulation promote a response through mechanosensory receptor complexes in the endothelial cells to release angiogenic factors, such as VEGF (Tzima et al., 2005), which are also essential for hematopoiesis. Therefore the absence of blood flow may impair both vasculogenesis and hematopoiesis. Nevertheless, the fact that placental vasculogenesis and hematopoiesis are initiated in *Ncx1*$^{-/-}$ embryos highlights the importance of the local signals in the placenta in induction of vessel formation and hematopoiesis.

The formation of hematopoietic cells from mesoderm demands specific signals from the surrounding microenvironment, including Indian Hedgehog (Ihh) and bone morphogenic protein 4 (BMP-4) (Baron, 2003). In the yolk sac, these signals arise from the visceral endoderm of the yolk sac, and in the embryo proper, from the visceral endoderm adjacent to the ventral side of the dorsal aorta. The avian allantois is known to have an endodermal component, whereas there is no evidence of an endodermal component in the mammalian allantois. Interestingly, the chorioallantoic mesenchyme of the placenta harbors endodermal structures known as Crypts of Duval (Figure 1) (Duval, 1891; Ogura et al., 1998). These structures express Ihh, whereas

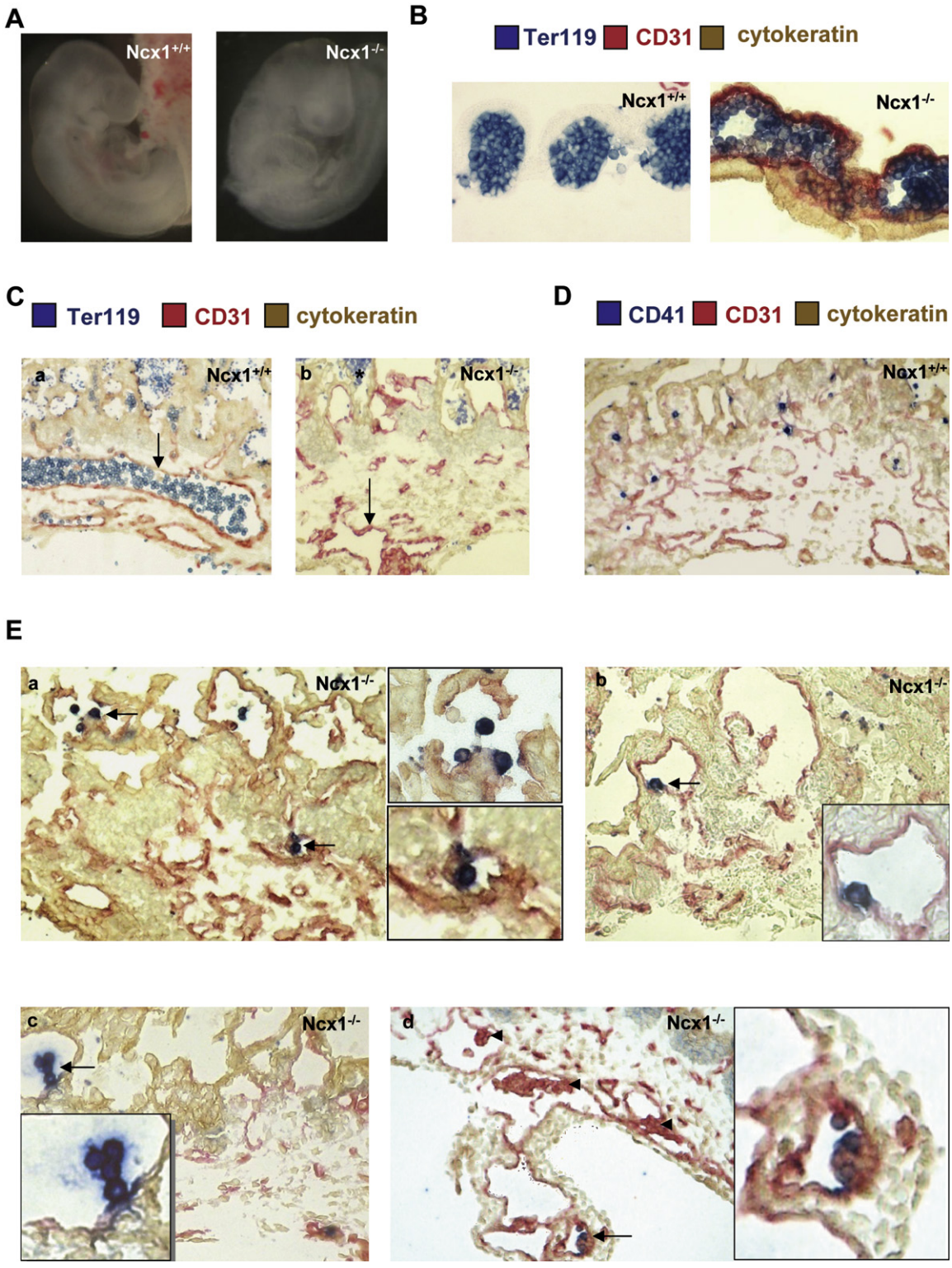

Figure 3. Definitive Hematopoietic Cells Emerge De Novo in Placental Vasculature in *Ncx1*$^{-/-}$ Mutants

(A) Images of embryos depict the absence of blood in the *Ncx1*$^{-/-}$ mutants due to the lack of circulation.

(B–E) Fixed frozen sections of E10.0 hematopoietic tissues stained with hematopoietic markers (blue), CD31 (endothelium, red), and cytokeratin (trophoblasts, brown).

(B) Yolk sac sections from both the *Ncx1*$^{+/+}$ and *Ncx1*$^{-/-}$ embryos show generation of Ter119+ primitive erythroblasts in yolk sac blood islands (100×). Note, in control yolk sac, only Ter119 staining is displayed.

the mesenchymal cells surrounding the crypts express Patched-1 (Ptch1), a receptor of Hedgehog signaling (Jiang and Herman, 2006). As the Crypts of Duval are in close proximity to the large vessels that generate HSCs, these endodermal structures may provide critical signals involved in the orchestration of HSC emergence in the placenta.

The timing of HSC emergence in the placenta, based on markers of developing HSCs in the vessels and appearance of first adult repopulating HSCs (Gekas et al., 2005), parallels that in the AGM, implying that hematopoiesis is initiated concomitantly in both sites. However, when the emergence of HSCs already ceases in the AGM, the number of adult repopulating HSCs in the placenta continues to increase (Gekas et al., 2005; Kumaravelu et al., 2002). Although both the AGM and the yolk sac possess HSC supportive capabilities, as evidenced by studies documenting that yolk sac and intraembryonic endothelial and stromal lines have the ability to maintain HSCs ex vivo (Li et al., 2003; Matsuoka et al., 2001; Oostendorp et al., 2002), lack of accumulation of a large pool of HSCs in vivo supports the hypothesis that these sites function in HSC generation rather than expansion. In comparison, in addition to the large chorioallantoic vessels where placental hematopoietic cells first emerge, the placenta contains another hematopoietic niche within the small vessels in the labyrinth. Presence of Runx1-lacZ+ hematopoietic clusters and colocalization of a mitosis marker with Runx1-lacZ+ cells in the placental vascular labyrinth suggest that, rather than simply providing a gateway for hematopoietic cells to pass through, the placental labyrinth may provide a microenvironment where definitive hematopoietic cells proliferate. The placental labyrinth has many unique features, such as the proximity of trophoblast cells, which release growth factors and cytokines, and influence from the maternal side that may contribute to its suitability as a hematopoietic niche. As the placenta is positioned between the dorsal aorta and the fetal liver in fetal circulation, the placental labyrinth may provide a transitory niche for HSCs generated in the placenta and other sites before liver colonization.

Analysis of the hematopoietic potential in extraembryonic and intraembryonic tissues in *Ncx1* mutants verified myeloid and lymphoid potential in not only the AGM and the placenta but also the yolk sac, suggesting that all three sites may independently generate HSCs. These data, combined with evidence from literature (Hadland et al., 2004; Lux et al., 2007; Palis et al., 1999), supports a model of at least three waves of hematopoiesis during embryogenesis. The first, primitive wave, occurs in the yolk sac, and generates a burst of primitive erythroid cells. The second wave, production of transient definitive progenitors, is initiated in the yolk sac, after which the progenitors circulate into the liver and give rise to definitive erythroid and myeloid cells that are the first mature blood cells released by the liver. The third wave, formation of HSCs, occurs in the large arteries and is not only confined to the AGM but also most likely occurs within the umbilical and vitelline arteries, the placenta, and the yolk sac (Figure 5). These programs are regulated in part by different mechanisms. As an example, Notch1 signaling is not required for generation of the primitive or the transient definitive progenitors in the yolk sac, but it is essential for formation of HSCs in the pSP/AGM (Hadland et al., 2004; Kumano et al., 2003). As hematopoietic cells from the distinct programs have different potential when placed in identical culture conditions or when transplanted into irradiated hosts, it is evident that cell-intrinsic regulatory mechanisms, including epigenetic modifications established during development, dictate the variable future developmental potential of these cells. However, far more needs to be learned about how these hematopoietic programs become segregated. Therefore, in order to generate HSCs de novo, for example from embryonic stem cells, it is critical that the correct microenvironmental cues are present from the beginning to secure the accurate developmental program toward self-renewing HSCs. The ability to recreate these developmental programs in vitro is dependent upon our success in defining these programs in vivo. Understanding how the major arterial regions generate HSCs and how these nascent hematopoietic cells are protected from premature differentiation in their native niches will be essential in advancing us toward this goal.

EXPERIMENTAL PROCEDURES

Mouse Models

Runx1-lacZ and *Runx1*$^{+/-}$ knockout mouse strains were obtained from Nancy Speck and Gary Gilliland (North et al., 1999; Wang et al., 1996), and *Runx1*-GFP mice (Figure S1) were from James Downing (Lorsbach et al., 2004). Timed matings were set up between *Runx1*$^{lacZ/+}$ males and *Runx1*$^{lacZ/+}$ or *Runx1*$^{+/-}$ females. *Runx1*$^{+/-}$ dams were used specifically to verify that lacZ+ cells are of fetal origin. The primers used for genotyping were as follows: lacZ F, 5′-TACCACAGC GGATGG TTCGG-3′ and R, 5′-GTGGTGGTTATGCCGATCGC-3′ (450 bp); Runx1-WT F, 5′-CACCTGTCTCTGCATCGCAGGACT-3′ and R, 5′-CCATCC GTGACAGATACGCAC CTC-3′ (450 bp); and Runx1-KO F, 5′-GAGTCCCAGCT GTCAATTCC-3′ and R, 5′-GGTGATGGTCAGAGTGAAGC-3′ (850 bp).

Ncx1 knockout mouse model was generated as described (Koushik et al., 2001) by inserting β-galactosidase gene into the *Ncx1* locus. Primers for genotyping were Ncx1 sense 5′-TGATGACCGGAGCTGGCAAC-3′ and antisense 5′-AGATCACAGTCCCTTCCGTG-3′ (300 bp) for the wild-type allele and the same lacZ primers listed above for the mutant allele.

To generate wild-type embryos, timed matings were set up between C57Bl/6 female and C57Bl/6.SJL male mice (Taconic, Oxnard, CA). All mice were maintained according to the guidelines of the UCLA Animal Research Committee.

Preparation of Paraffin-Embedded Tissue Sections

In experiments with *Runx1*-lacZ mouse model, β-galactosidase staining was performed according to the manufacturer's protocol (Chemicon) prior to preparation of the paraffin blocks and tissue sections. Subsequently, fetal hematopoietic tissues were fixed in formalin (10% Buffered Formalin, Fisher) at room temperature for 24 hr. After rinsing with running tap water for 15 min, tissues were transferred to 70% ETOH. Small tissues from younger embryos were embedded in Histogel (Richard Allan Scientific). Paraffin blocks were made

(C) (a) Fetal vessels (arrow) were filled with Ter119+ red cells in the *Ncx1*$^{+/+}$ placenta, whereas (b) the vessels (arrow) in *Ncx1*$^{-/-}$ placentas were empty. The asterisk (*) indicates *Ncx1*$^{-/-}$ placentas that did harbor maternal Ter119+ cells within the trophoblast lined maternal blood spaces (20×).
(D) An *Ncx1*$^{+/+}$ control placenta stained with CD41 documents localization of definitive hematopoietic cells (20×).
(E) (a–d) *Ncx1*$^{-/-}$ placentas demonstrate the emergence of CD41+ cells (arrows) in placental vasculature in the absence of blood flow (40×, insets 100×). Arrowhead marks unique CD31+ aggregates in the placenta (20×, inset 100×). (d) Arrow and inset show CD31+CD41+/− aggregate in the umbilical cord of an *Ncx1*$^{-/-}$ embryo.

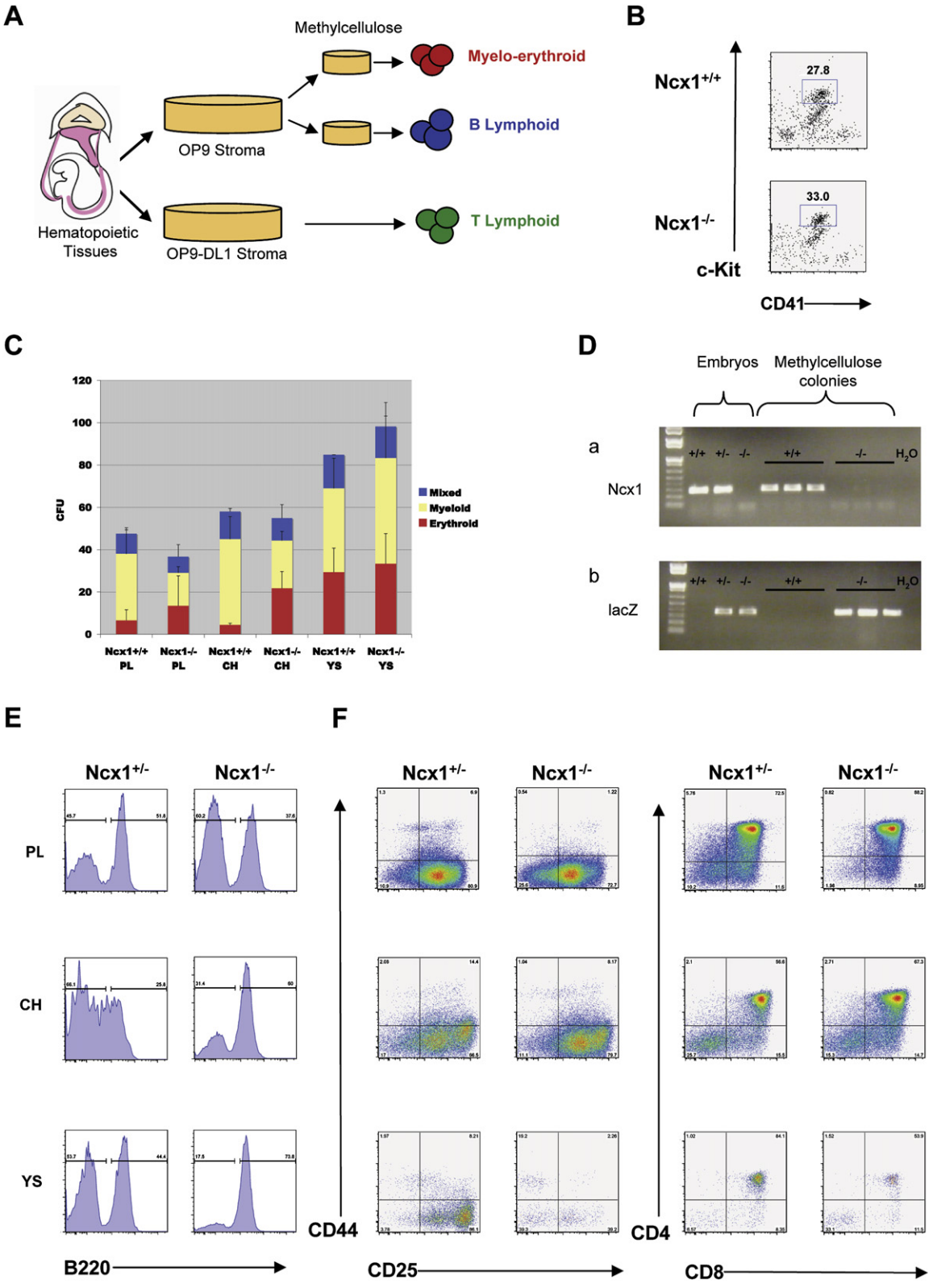

Figure 4. Definitive Hematopoietic Cells Derived from *Ncx1*$^{-/-}$ Placentas Have Myelo-Erythroid and Lymphoid Potential

(A) Placenta, yolk sac, and caudal half of the embryos were dissected, and the tissue explants were cultured on OP9 and OP9-DL1 stroma. Myelo-erythroid and B lymphoid potential was assessed after plating of the cells from the OP9 stroma on methylcellulose culture, whereas T lymphoid potential was assessed directly on OP9-DL1 stroma.

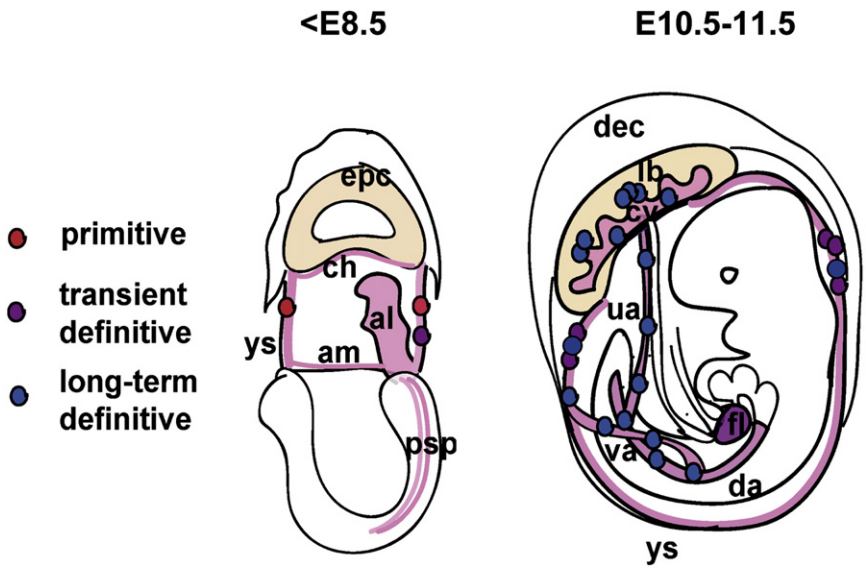

Figure 5. Revised Model of Embryonic Hematopoietic Sites

Fetal hematopoiesis can be divided into at least three different waves. The first waves of hematopoiesis occur in the yolk sac: the primitive wave, which gives rise to primitive erythroblasts, and the transient definitive wave, which generates myelo-erythroid progenitors that first colonize the liver. In contrast, the emergence of adult repopulating HSCs occurs in multiple sites yet is confined to the major blood vessels: the dorsal aorta, the adjacent vitelline, umbilical vessels. and as shown in this study, the large vessels of the placenta. Subsequently, HSCs generated in the placenta and possibly the AGM and yolk sac are directed via blood flow to the placental labyrinth, which may provide a unique environment for HSC expansion/maturation prior to seeding of the fetal liver. Pink marks mesodermal tissues with hematopoietic potential (al, allantois; ch, chorion; ys, yolk sac; and p-sp, para-aortic splanchopleura) and their derivatives (ua, umbilical artery; cv, chorio-allantoic vessels; va, vitelline artery; and da, dorsal aorta), and brown marks trophoectodermal tissues (epc, ectoplacental cone and lb, placental labyrinth). Dec, maternal decidua and fl, fetal liver.

by standard protocol at the Tissue Procurement and Histology Core Laboratory, Pathology and Laboratory Medicine at UCLA and cut into 5 μm sections.

Preparation of Frozen Tissue Sections

Tissues were isolated in cold 1× PBS and fixed in 4% PFA (Electron Microscopy Sciences diluted) for 4–6 hr, followed by equilibration in 30% sucrose in PBS solution overnight. The tissues were placed in 1:1 30% sucrose/OCT solution for 1–2 hr, in 100% OCT (Tissue-Tek, Electron Microscopy Sciences) for 1 hr at 4°C, and embedded in 100% OCT, carefully oriented in Cryomold (Tissue Tek). The blocks were frozen on dry ice and stored at −80°C. The sections were cut 7–10 μm with a Leica CM3050 S cryostat.

Immunohistochemistry on Paraffin Sections

Paraffin sections were stained with primary antibodies that identify key cell types in the placenta: polyclonal rabbit anti-laminin for mesodermal derivatives in the placenta (1:600, DakoCytomation) and polyclonal rabbit anti-cow pan-cytokeratin for trophoblasts and epithelium (1:1000, DakoCytomation). Proteinase K treatment (100 μg/ml, 10 min) was used for antigen retrieval in most experiments, whereas TRIS-EDTA (pH 9.0) treatment was performed prior to pH3S10 staining. Biotinylated anti-rabbit IgG secondary antibody (1:1000,Vector) was used in conjunction with laminin, cytokeratin, and PH3S10. Immunohistochemistry was performed according to standard protocols with the Vectastain ABC kit for DAB (brown) and Vector VIP (dark purple/brown) and Vectastain ABC-AP kit for Vector Red and Vector Blue (Vector).

Immunohistochemistry on Fixed Frozen Sections

A modified standard staining protocol was used for fixed frozen sections. The sections were treated with 2.5 μg/ml of Proteinase K for 10 min. Primary antibodies, CD41 (1:50 BD PharMingen), CD45 (1:50 BD PharMingen), Mac1 (1:200 BD PharMingen), F4/80 (1:200 eBioscience), and PECAM-1/CD31 (1:200, BD PharMingen) were used on fixed frozen sections with Tyramide (Invitrogen) amplification according to the manufacturer's protocol. Ter119 (1:50 eBioscience) and cytokeratin (1:1000 DakoCytomation) were used without Tyramide amplification. Biotinylated anti-rabbit IgG (1:1000,Vector) was used as a secondary antibody for cytokeratin, whereas biotinylated anti-rat IgG (1:1000, Vector) was used for all other primary antibodies.

Flow Cytometry and Cell Sorting

Flow cytometry was performed by rat anti-mouse monoclonal antibodies against c-Kit, CD41, CD34, Sca1, Mac-1, Gr-1, B220, CD19, CD44, CD25, CD4, CD8 (BD Bioscience) F4/80, and CD45 (eBioscience). Dead cells were excluded with 7AAD staining (BD PharMingen). Cells were assayed on a BD LSRII flow cytometer and data were analyzed with FlowJo software (Tree Star Inc., Ashland, OR). Hematopoietic tissues from E10–11 embryos were fractionated into CD41+ and CD41− populations by BD FACS Aria and BD FACS Vantage sorter, and developmental potential of the sorted cells was assayed on OP9 stroma and methylcellulose cultures.

OP9 and OP9-DL1 Explant Cultures

Fetal organ explants were cocultured on mouse OP9 stromal cells in 24-well plates in 1 ml α-MEM (GIBCO/Invitrogen) containing 20% fetal bovine serum (Hyclone), 1% penicillin/streptomycin and supplemented with stem cell factor (SCF, 50 ng/ml), interleukin-3 (IL3, 5 ng/ml), interleukin-6 (IL6, 5 ng/ml), Thrombopoietin (TPO, 5 ng/ml), interleukin 7 (IL-7, 10 ng/ml), and Flt-3 Ligand (Flt-3L, 10 ng/ml) for 4 days. Half of the medium with cytokines was replaced every other day. To assay B lymphoid potential, explants were replated on fresh

(B) Flow cytometry reveals robust generation of c-Kit+CD41+ definitive progenitors from E8.5 *Ncx1*$^{+/+}$ and *Ncx1*$^{-/-}$ placentas during OP9 coculture.
(C) Analysis of myelo-erythroid colonies differentiated on methylcellulose after OP9 coculture reveals development of mixed, myeloid, and erythroid colonies from *Ncx1*$^{-/-}$ and control tissues. Colonies are derived from 0.2 embryo equivalents of tissue. Error bars represent the standard deviation.
(D) PCR analysis of individual colonies derived from *Ncx1*$^{+/+}$ and *Ncx1*$^{-/-}$ placentas documents fetal origin of the colonies. (a) PCR for Ncx1 wild-type allele, (b) PCR for Ncx1-lacZ allele. Three colonies of each genotype are shown of 20 total colonies/genotype that were analyzed. Maternal colonies (*Ncx1*$^{+/-}$) were never observed.
(E) Flow cytometry of hematopoietic cells differentiated on methylcellulose after OP9 coculture shows B220+ B lymphoid cells derived from placenta, yolk sac, and caudal half tissues of control and *Ncx1*$^{-/-}$ embryos. Plots from a representative experiment of four total experiments are shown.
(F) Flow cytometry performed after explant culture on OP9-DL1 stroma documents robust T cell potential in *Ncx1*$^{+/+}$ and *Ncx1*$^{-/-}$ embryos in all hematopoietic tissues. Both immature T lymphoid precursors (CD44+/−CD25+/−) and more mature T cells (CD4+/−CD8+/−) were observed. Total of three experiments were performed, and representative plots are shown.

OP9 stromal cells and grown in the same media but supplemented with B cell promoting cytokines only: IL7 (100 ng/ml), SCF (50 ng/ml), and Flt-3L (40 ng/ml).

To investigate T lymphoid potential, tissue explants were plated directly on OP9-DL1 stroma and supplemented with TPO (5 ng/ml), IL7 (1 ng/ml), SCF (50 ng/ml), and Flt-3L (5 ng/ml). After 4 days of culture, TPO was withdrawn. T lymphoid differentiation was assessed after 10–15 days of culture.

Colony-Forming Assays

To determine myelo-erythroid potential of the tissues, explants were dissociated mechanically after 4 days of OP9 coculture and plated on 1.5 ml methylcellulose with SCF, IL-6, IL-3, and EPO (MethoCult 3434, Stem Cell Technologies) supplemented by TPO (5 ng/ml). Colonies were scored 6–8 days later. In *Ncx1*$^{-/-}$ experiments, individual colonies were genotyped by PCR to verify fetal identity of the hematopoietic colonies.

To assay B cell maturation, after 6–10 days of OP9 culture in B cell promoting conditions, cells were plated on B lymphoid methylcellulose assay supplemented with IL7 (100 ng/ml), SCF (50 ng/ml), and Flt-3L (40 ng/ml), harvested after 14–17 days, and analyzed by flow cytometry. B cell identity was confirmed by IgH D-J rearrangement PCR as previously described (Ehlich et al., 1994) and verified by sequencing by the UCLA Sequencing and Genotyping Core Facility following gel extraction (QIAquick Gel Extraction Kit, QIAGEN).

SUPPLEMENTAL DATA

Supplemental Data include three figures and can be found with this article online at http://www.cellstemcell.com/cgi/content/full/2/3/252/DC1/.

ACKNOWLEDGMENTS

We thank Nancy Speck for providing the *Runx1*-lacZ *and Runx1*$^{+/-}$ mouse strains and Jim Downing for the *Runx1*-GFP strain. We thank Hildur Helgadottir and Joanna Gallino for assistance with mouse breeding, the Tissue Procurement Laboratory at UCLA for processing paraffin sections, and Eija Hamalainen and Sharina Palencia-Desai for assistance in setting up Immunohistochemistry. We thank Encarnacion Montecino-Rodriguez for her expert advice on B cell differentiation and Juan Carlos Zuñiga-Pflücker for providing the OP9-Dl1 stroma line. We thank William Lowry for critically reading the manuscript. We acknowledge Francoise Dieterlen-Lievre for her original idea and inspiration to investigate hematopoiesis in the placenta. This work was supported by grants from NIH DK069659, Harvard Stem Cell Institute, and American Society of Hematology to H.K.A.M. and NIH HL63169 for M.C.Y. K.E.R. was supported by a Ruth L. Kirschstein National Research Service Award GM07185 at UCLA.

Received: September 18, 2007
Revised: December 10, 2007
Accepted: January 2, 2008
Published: March 5, 2008

REFERENCES

Adams, G.B., and Scadden, D.T. (2006). The hematopoietic stem cell in its place. Nat. Immunol. *7*, 333–337.

Alvarez-Silva, M., Belo-Diabangouaya, P., Salaun, J., and Dieterlen-Lievre, F. (2003). Mouse placenta is a major hematopoietic organ. Development *130*, 5437–5444.

Baron, M.H. (2003). Embryonic origins of mammalian hematopoiesis. Exp. Hematol. *31*, 1160–1169.

Bertrand, J.Y., Giroux, S., Golub, R., Klaine, M., Jalil, A., Boucontet, L., Godin, I., and Cumano, A. (2005). Characterization of purified intraembryonic hematopoietic stem cells as a tool to define their site of origin. Proc. Natl. Acad. Sci. USA *102*, 134–139.

Bordignon, C. (2006). Stem-cell therapies for blood diseases. Nature *441*, 1100–1102.

Bowie, M.B., McKnight, K.D., Kent, D.G., McCaffrey, L., Hoodless, P.A., and Eaves, C.J. (2006). Hematopoietic stem cells proliferate until after birth and show a reversible phase-specific engraftment defect. J. Clin. Invest. *116*, 2808–2816.

Cai, Z., de Bruijn, M., Ma, X., Dortland, B., Luteijn, T., Downing, R.J., and Dzierzak, E. (2000). Haploinsufficiency of AML1 affects the temporal and spatial generation of hematopoietic stem cells in the mouse embryo. Immunity *13*, 423–431.

Cairo, M.S., and Wagner, J.E. (1997). Placental and/or umbilical cord blood: an alternative source of hematopoietic stem cells for transplantation. Blood *90*, 4665–4678.

Caprioli, A., Jaffredo, T., Gautier, R., Dubourg, C., and Dieterlen-Lievre, F. (1998). Blood-borne seeding by hematopoietic and endothelial precursors from the allantois. Proc. Natl. Acad. Sci. USA *95*, 1641–1646.

Caprioli, A., Minko, K., Drevon, C., Eichmann, A., Dieterlen-Lievre, F., and Jaffredo, T. (2001). Hemangioblast commitment in the avian allantois: cellular and molecular aspects. Dev. Biol. *238*, 64–78.

Corbel, C., and Salaun, J. (2002). AlphaIIb integrin expression during development of the murine hemopoietic system. Dev. Biol. *243*, 301–311.

Corbel, C., Salaun, J., Belo-Diabangouaya, P., and Dieterlen-Lievre, F. (2007). Hematopoietic potential of the pre-fusion allantois. Dev. Biol. *301*, 478–488.

Cross, J.C. (2005). How to make a placenta: mechanisms of trophoblast cell differentiation in mice–a review. Placenta *26* (*Suppl A*), S3–S9.

Cumano, A., Dieterlen-Lievre, F., and Godin, I. (1996). Lymphoid potential, probed before circulation in mouse, is restricted to caudal intraembryonic splanchnopleura. Cell *86*, 907–916.

de Bruijn, M.F., Speck, N.A., Peeters, M.C., and Dzierzak, E. (2000). Definitive hematopoietic stem cells first develop within the major arterial regions of the mouse embryo. EMBO J. *19*, 2465–2474.

Duval, M. (1891). Le placenta des rongeurs. J. Anat. Physiol. *27*, 24–73, 344–395, 513–612.

Ehlich, A., Martin, V., Muller, W., and Rajewsky, K. (1994). Analysis of the B-cell progenitor compartment at the level of single cells. Curr. Biol. *4*, 573–583.

Ferkowicz, M.J., Starr, M., Xie, X., Li, W., Johnson, S.A., Shelley, W.C., Morrison, P.R., and Yoder, M.C. (2003). CD41 expression defines the onset of primitive and definitive hematopoiesis in the murine embryo. Development *130*, 4393–4403.

Fraser, S.T., Ogawa, M., Yu, R.T., Nishikawa, S., Yoder, M.C., and Nishikawa, S. (2002). Definitive hematopoietic commitment within the embryonic vascular endothelial-cadherin(+) population. Exp. Hematol. *30*, 1070–1078.

Gekas, C., Dieterlen-Lievre, F., Orkin, S.H., and Mikkola, H.K. (2005). The placenta is a niche for hematopoietic stem cells. Dev. Cell *8*, 365–375.

Hadland, B.K., Huppert, S.S., Kanungo, J., Xue, Y., Jiang, R., Gridley, T., Conlon, R.A., Cheng, A.M., Kopan, R., and Longmore, G.D. (2004). A requirement for Notch1 distinguishes 2 phases of definitive hematopoiesis during development. Blood *104*, 3097–3105.

Inman, K.E., and Downs, K.M. (2007). The murine allantois: emerging paradigms in development of the mammalian umbilical cord and its relation to the fetus. Genesis *45*, 237–258.

Jaffredo, T., Nottingham, W., Liddiard, K., Bollerot, K., Pouget, C., and de Bruijn, M. (2005). From hemangioblast to hematopoietic stem cell: an endothelial connection? Exp. Hematol. *33*, 1029–1040.

Jiang, F., and Herman, G.E. (2006). Analysis of Nsdhl-deficient embryos reveals a role for Hedgehog signaling in early placental development. Hum. Mol. Genet. *15*, 3293–3305.

Kiel, M.J., and Morrison, S.J. (2006). Maintaining hematopoietic stem cells in the vascular niche. Immunity *25*, 862–864.

Kim, I., Saunders, T.L., and Morrison, S.J. (2007). Sox17 dependence distinguishes the transcriptional regulation of fetal from adult hematopoietic stem cells. Cell *130*, 470–483.

Koushik, S.V., Wang, J., Rogers, R., Moskophidis, D., Lambert, N.A., Creazzo, T.L., and Conway, S.J. (2001). Targeted inactivation of the sodium-calcium exchanger (Ncx1) results in the lack of a heartbeat and abnormal myofibrillar organization. FASEB J. *15*, 1209–1211.

Kumano, K., Chiba, S., Kunisato, A., Sata, M., Saito, T., Nakagami-Yamaguchi, E., Yamaguchi, T., Masuda, S., Shimizu, K., Takahashi, T., et al. (2003). Notch1 but not Notch2 is essential for generating hematopoietic stem cells from endothelial cells. Immunity *18*, 699–711.

Kumaravelu, P., Hook, L., Morrison, A.M., Ure, J., Zhao, S., Zuyev, S., Ansell, J., and Medvinsky, A. (2002). Quantitative developmental anatomy of definitive haematopoietic stem cells/long-term repopulating units (HSC/RUs): role of the aorta-gonad-mesonephros (AGM) region and the yolk sac in colonisation of the mouse embryonic liver. Development *129*, 4891–4899.

Lessard, J., Faubert, A., and Sauvageau, G. (2004). Genetic programs regulating HSC specification, maintenance and expansion. Oncogene *23*, 7199–7209.

Li, W., Johnson, S.A., Shelley, W.C., Ferkowicz, M., Morrison, P., Li, Y., and Yoder, M.C. (2003). Primary endothelial cells isolated from the yolk sac and para-aortic splanchnopleura support the expansion of adult marrow stem cells in vitro. Blood *102*, 4345–4353.

Lorsbach, R.B., Moore, J., Ang, S.O., Sun, W., Lenny, N., and Downing, J.R. (2004). Role of RUNX1 in adult hematopoiesis: analysis of RUNX1-IRES-GFP knock-in mice reveals differential lineage expression. Blood *103*, 2522–2529.

Lux, C.T., Yoshimoto, M., McGrath, K., Conway, S.J., Palis, J., and Yoder, M.C. (2007). All primitive and definitive hematopoietic progenitor cells emerging prior to E10 in the mouse embryo are products of the yolk sac. Blood Press. Published online October 11, 2007. 10.1182/blood-2007-08-107086.

Martinez-Agosto, J.A., Mikkola, H.K., Hartenstein, V., and Banerjee, U. (2007). The hematopoietic stem cell and its niche: a comparative view. Genes Dev. *21*, 3044–3060.

Matsubara, A., Iwama, A., Yamazaki, S., Furuta, C., Hirasawa, R., Morita, Y., Osawa, M., Motohashi, T., Eto, K., Ema, H., et al. (2005). Endomucin, a CD34-like sialomucin, marks hematopoietic stem cells throughout development. J. Exp. Med. *202*, 1483–1492.

Matsuoka, S., Tsuji, K., Hisakawa, H., Xu, M., Ebihara, Y., Ishii, T., Sugiyama, D., Manabe, A., Tanaka, R., Ikeda, Y., et al. (2001). Generation of definitive hematopoietic stem cells from murine early yolk sac and paraaortic splanchnopleures by aorta-gonad-mesonephros region-derived stromal cells. Blood *98*, 6–12.

McGrath, K.E., Koniski, A.D., Malik, J., and Palis, J. (2003). Circulation is established in a stepwise pattern in the mammalian embryo. Blood *101*, 1669–1676.

McKinney-Freeman, S.L., and Daley, G.Q. (2007). Towards hematopoietic reconstitution from embryonic stem cells: a sanguine future. Curr. Opin. Hematol. *14*, 343–347.

Medvinsky, A., and Dzierzak, E. (1996). Definitive hematopoiesis is autonomously initiated by the AGM region. Cell *86*, 897–906.

Melchers, F. (1979). Murine embryonic B lymphocyte development in the placenta. Nature *277*, 219–221.

Mikkola, H.K., and Orkin, S.H. (2006). The journey of developing hematopoietic stem cells. Development *133*, 3733–3744.

Mikkola, H.K., Fujiwara, Y., Schlaeger, T.M., Traver, D., and Orkin, S.H. (2003). Expression of CD41 marks the initiation of definitive hematopoiesis in the mouse embryo. Blood *101*, 508–516.

Mitjavila-Garcia, M.T., Cailleret, M., Godin, I., Nogueira, M.M., Cohen-Solal, K., Schiavon, V., Lecluse, Y., Le Pesteur, F., Lagrue, A.H., and Vainchenker, W. (2002). Expression of CD41 on hematopoietic progenitors derived from embryonic hematopoietic cells. Development *129*, 2003–2013.

North, T., Gu, T.L., Stacy, T., Wang, Q., Howard, L., Binder, M., Marin-Padilla, M., and Speck, N.A. (1999). Cbfa2 is required for the formation of intra-aortic hematopoietic clusters. Development *126*, 2563–2575.

North, T.E., de Bruijn, M.F., Stacy, T., Talebian, L., Lind, E., Robin, C., Binder, M., Dzierzak, E., and Speck, N.A. (2002). Runx1 expression marks long-term repopulating hematopoietic stem cells in the midgestation mouse embryo. Immunity *16*, 661–672.

Ogura, Y., Takakura, N., Yoshida, H., and Nishikawa, S.I. (1998). Essential role of platelet-derived growth factor receptor alpha in the development of the intraplacental yolk sac/sinus of Duval in mouse placenta. Biol. Reprod. *58*, 65–72.

Oostendorp, R.A., Harvey, K.N., Kusadasi, N., de Bruijn, M.F., Saris, C., Ploemacher, R.E., Medvinsky, A.L., and Dzierzak, E.A. (2002). Stromal cell lines from mouse aorta-gonads-mesonephros subregions are potent supporters of hematopoietic stem cell activity. Blood *99*, 1183–1189.

Ottersbach, K., and Dzierzak, E. (2005). The murine placenta contains hematopoietic stem cells within the vascular labyrinth region. Dev. Cell *8*, 377–387.

Palis, J., Robertson, S., Kennedy, M., Wall, C., and Keller, G. (1999). Development of erythroid and myeloid progenitors in the yolk sac and embryo proper of the mouse. Development *126*, 5073–5084.

Schmitt, T.M., and Zuniga-Pflucker, J.C. (2002). Induction of T cell development from hematopoietic progenitor cells by delta-like-1 in vitro. Immunity *17*, 749–756.

Suda, T., Arai, F., and Hirao, A. (2005). Hematopoietic stem cells and their niche. Trends Immunol. *26*, 426–433.

Taoudi, S., Morrison, A.M., Inoue, H., Gribi, R., Ure, J., and Medvinsky, A. (2005). Progressive divergence of definitive haematopoietic stem cells from the endothelial compartment does not depend on contact with the foetal liver. Development *132*, 4179–4191.

Teitell, M.A., and Mikkola, H.K. (2006). Transcriptional activators, repressors, and epigenetic modifiers controlling hematopoietic stem cell development. Pediatr. Res. *59*, 33R–39R.

Tzima, E., Irani-Tehrani, M., Kiosses, W.B., Dejana, E., Schultz, D.A., Engelhardt, B., Cao, G., DeLisser, H., and Schwartz, M.A. (2005). A mechanosensory complex that mediates the endothelial cell response to fluid shear stress. Nature *437*, 426–431.

Wang, Q., Stacy, T., Binder, M., Marin-Padilla, M., Sharpe, A.H., and Speck, N.A. (1996). Disruption of the Cbfa2 gene causes necrosis and hemorrhaging in the central nervous system and blocks definitive hematopoiesis. Proc. Natl. Acad. Sci. USA *93*, 3444–3449.

Weissman, I.L. (2000). Stem cells: units of development, units of regeneration, and units in evolution. Cell *100*, 157–168.

Wilson, A., and Trumpp, A. (2006). Bone-marrow haematopoietic-stem-cell niches. Nat. Rev. Immunol. *6*, 93–106.

Yoder, M.C., Hiatt, K., Dutt, P., Mukherjee, P., Bodine, D.M., and Orlic, D. (1997a). Characterization of definitive lymphohematopoietic stem cells in the day 9 murine yolk sac. Immunity *7*, 335–344.

Yoder, M.C., Hiatt, K., and Mukherjee, P. (1997b). In vivo repopulating hematopoietic stem cells are present in the murine yolk sac at day 9.0 postcoitus. Proc. Natl. Acad. Sci. USA *94*, 6776–6780.

Zeigler, B.M., Sugiyama, D., Chen, M., Guo, Y., Downs, K.M., and Speck, N.A. (2006). The allantois and chorion, when isolated before circulation or chorioallantoic fusion, have hematopoietic potential. Development *133*, 4183–4192.

Zhang, J., Niu, C., Ye, L., Huang, H., He, X., Tong, W.G., Ross, J., Haug, J., Johnson, T., Feng, J.Q., et al. (2003). Identification of the haematopoietic stem cell niche and control of the niche size. Nature *425*, 836–841.